Broadband Dual-Use Array with Planar Log Periodic Dipole Elements

Seth A. McCormick and William O. Coburn

Army Research Laboratory
Adelphi, Maryland 20783, United States of America
seth.a.mccormick.civ@mail.mil, william.o.coburn.civ@mail.mil

Abstract — This paper presents a phased array consisting of 8 horizontally positioned planar log periodic dipole array antennas for use over the frequency range of 800 to 1,300 MHz. The array is dual use in that it can either scan in azimuth with a narrow beam or be forward looking with a null-filled broad beam. To achieve the broad beam, the 8-element array is divided into two 4-element subarrays. The main beam of each subarray is then pointed near the first null of the 8-element uniform array radiation pattern to "fill" the nulls. The results for the narrow beam configuration produce an azimuthal beamwidth of 15° with 15 dBi of gain, and the null-filled configuration produces an increase in azimuthal beamwidth to 55° (40° increase) with a peak gain of 10 dBi (loss of 5 dB). Note that this paper only presents the antenna development and array testing but not any system hardware.

Index Terms — Antipodal antennas, null filling, phased arrays, planar log periodic dipole array, sub arrays.

I. INTRODUCTION

Achieving high gain with a relatively broad beamwidth can be a challenge for antenna engineers. Given the inverse relationship between gain and beamwidth, where a large gain implies a small beamwidth and vice versa, the antenna engineer must prioritize one or accept a middle ground for both (or change the beamwidth criterion from 3 dB). Still, designing a single antenna element that meets both gain and broad beam requirements can be a challenge as the radiation pattern cannot be easily manipulated.

For phased arrays, however, the radiation pattern can be easily manipulated and thus generate a high gain, broad beam radiating aperture. In phased arrays, the radiated phase front can be electronically controlled, thereby steering the beam to any forward location in azimuth and elevation given a sufficient number of elements. With the ability to manipulate the shape of the beam, it is possible to maximize both beamwidth and gain with a phased array system by sub-dividing the array into scanned subarrays. The subarrays can then point to near the first null of the uniform array pattern, filling the nulls, thereby broadening the beam. Similar methods are seen in pattern synthesis and is typically called null filling [1], but for the presented array, null filling will refer to the first nulls of the combined array pattern instead of just locations of lost coverage [2].

This paper describes the design of planar log periodic dipole array (LPDA) antenna elements for use in a dual function array. The antennas and array are designed and evaluated using FEKO [3], a commercial computational electromagnetics (CEM) code using the Method of Moments (MoM). The frequency band to be covered is 800 to 1,300 MHz. The 8-element array must be able to scan in azimuth for one configuration, and must maximize both forward gain and azimuthal beamwidth in the other configuration.

Several design variations of the antenna and array were examined with the final design being an 8-element horizontal array. The development of the antenna elements and testing of the scanning and null filling are presented in the next two sections.

II. PLANAR LOG PERIODIC DIPOLE ARRAY ELEMENT

An LPDA element is chosen to obtain the required gain-bandwidth product. The conventional LPDA is a linear array of parallel dipoles with unequal lengths, L_n, widths, w_n and spacing, d_n, fed by a twisted transmission line [4]. A planar version is designed that exceeds the bandwidth requirement having scale factor $\tau = l_{n+1}/l_n = w_{n+1}/w_n = d_{n+1}/d_n$ = 0.9 with 14 dipole elements [5]. It has total length, L = 335.5 mm, and total width, W = 322.3 mm not including the substrate where L is the full array length and W would correspond to the longest dipole length including the center trace width.

A compact version is designed to minimize length by linearly scaling the entire structure by 2/3 which increases the gain at the highest frequencies. The surface current distribution at 900 MHz is compared in Fig. 1, indicating that the original design radiates from the smaller dipoles so is approaching the end of its frequency bandwidth. This planar LPDA has 14 antipodal dipole elements with total length L = 223.6 mm and W = 210.7 mm without substrate. Including the substrate, the total length and

Submitted On: May 26, 2016
Accepted On: August 16, 2017

width are 239.3 mm and 232.7 mm respectively. Both use 1.57 mm substrate thickness where the center trace is 4.15 mm in width. This trace width is not included in the antipodal dipole arm lengths. The first dipole, which sets the low frequency as $l_1 \approx \frac{\lambda_L}{2}$ = 686 MHz, has dimensions $l_1 = 210.85$ mm and $w_1 = 7.16$ mm for the compact design with a center spacing to the next dipole of $d_1 = 28.32$ mm. Following a linear scale, the next element length would be $l_2 = \tau l_1 = 189.77$ mm and width would be $w_2 = \tau w_1 = 6.44$ mm with next dipole spacing $d_2 = \tau d_1 = 25.49$ mm.

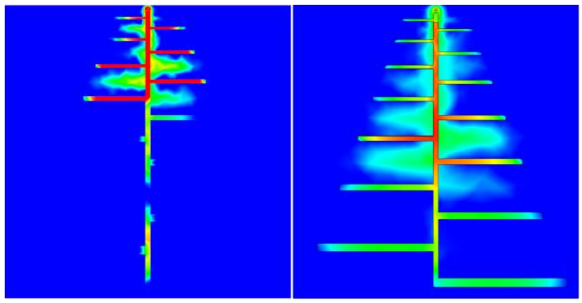

Fig. 1. Planar LPDA antenna elements top view (left) original and (right) compact design, not to scale.

Additional design approaches investigated included variations in the trace and pin-feed connection at the tip of the planar LPDA. Various configurations of the feed cable were considered but not included in the model, with one example shown in Fig. 2. This investigation determined that contrary to what is typically found in the literature, electrical connections of the cable shield to the trace degraded performance, so an insulated cable was subsequently used. This was found for either spot or continuous solder joints.

The cable shield is connected only at the tip of the trace and insulated with a Kapton thin film over its length. This final feed point design was modeled with a short section of coaxial cable with a waveguide port. A finer mesh is used on the feed where the center conductor is modeled as a cylinder connected to the bottom trace. A cylinder was used instead of a wire because of the thin wire limitation in MoM where the segment to radius ratio was too large to mesh the actual center conductor. The dielectric extending from the cable shield (see Fig. 2) was included with negligible difference. This model was sufficient to represent the feed point to obtain an accurate input impedance.

The simulation required 1.7 GB and 0.1 hours per frequency on 4 CPUs. The result for this initial LPDA on Duroid is shown in Fig. 3 for the measured reflection coefficient compared to the simulated result. The agreement between simulation and measurement is fair, justifying the chosen feed model.

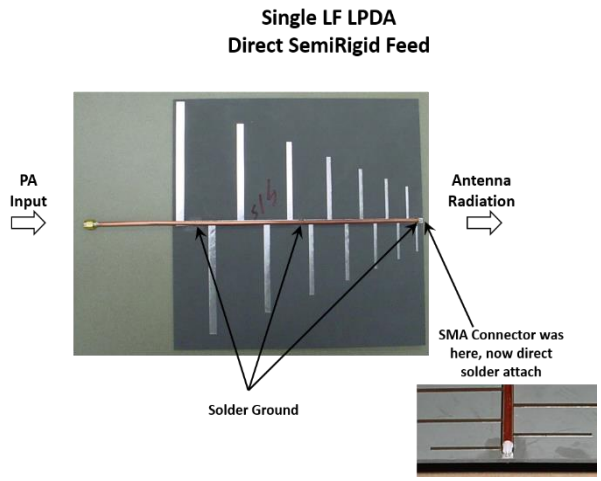

Fig. 2. Planar LPDA initial fabrication.

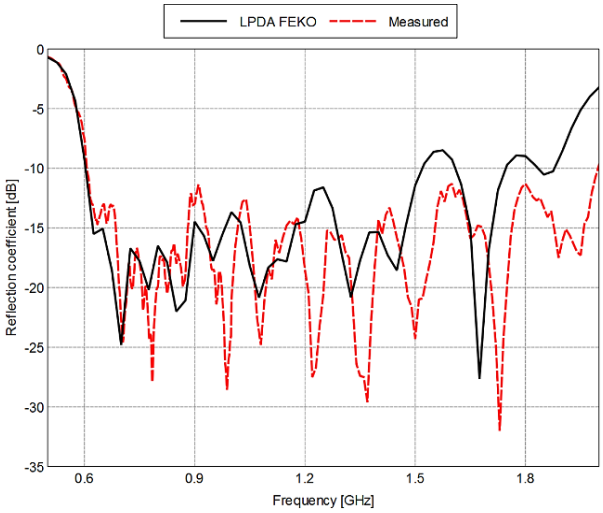

Fig. 3. Planar compact LPDA on Duroid reflection coefficient comparison.

The final planar LPDA design was slightly longer to accommodate a longer trace for the pin-feed connection at the tip of the antenna. The dipole arms were also rounded at the tips. The feed cable was routed along but insulated from the center trace. The final result for the planar LPDA on Duroid is shown in Fig. 4 and Fig. 5 for the measured reflection coefficient and gain compared to the simulation results respectively. A commercial time-domain finite-difference (TDFD) solver, GEMS [6], was used for code-to-code validation. The time-domain solver is more efficient to capture the measured oscillations in the reflection coefficient compared to the large number of frequencies that would be required in the frequency domain. The E-plane pattern comparison is shown in Fig. 6 at 900 and 1300 MHz where the simulation and measurement are in agreement except in the backlobe.

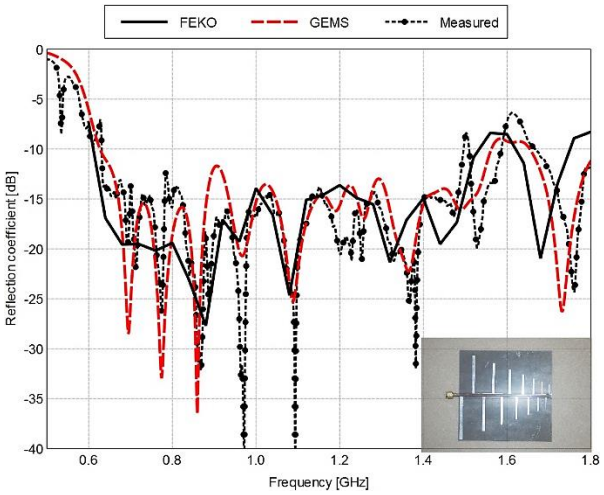

Fig. 4. Planar LPDA reflection coefficient comparison.

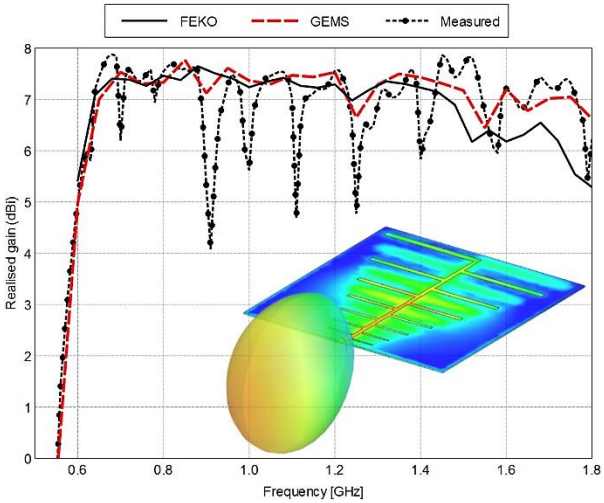

Fig. 5. Planar compact LPDA gain comparison.

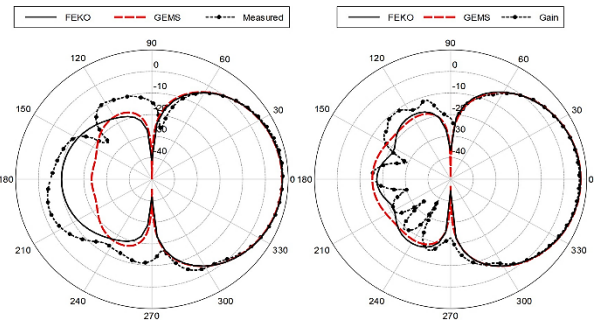

Fig. 6. Planar LPDA E-plane radiation pattern at (left) 900 MHz and (right) 1300 MHz.

The cost of fabricating the planar LPDA elements on Duroid was a concern, so FR4, a flame resistance glass reinforced epoxy laminate, was chosen as the final substrate to reduce cost. The higher loss substrate ($\tan\delta = 0.02$) produced a ~1.7 dB gain penalty compared to using the much lower loss ($\tan\delta = 0.001$) RT/Duroid® 5880 laminates. The planar design on FR4 vs. Duroid substrates will have roughly an order of magnitude lower fabrication cost but with a significant gain penalty.

With Duroid, the compact LPDA has similar gain as the original antenna but with a 10 dB larger back lobe. The FR4 version has at least 1.6 dB less gain but a 10 dB lower back lobe. The boresight gain versus frequency is shown in Fig. 7 where the original LPDA has reduced gain above 1200 MHz. The compact design meets the bandwidth requirement although the FR4 version has reduced gain. The measured gain for the prototypes has some artifacts associated with noise limitations in the anechoic chamber measurements.

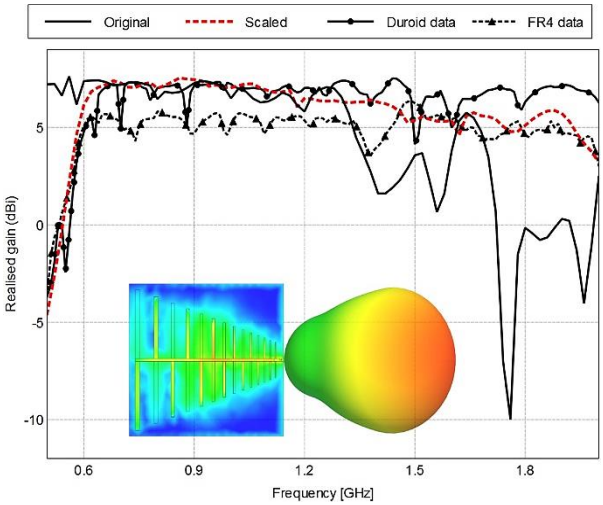

Fig. 7. Simulated boresight gain versus frequency compared to the measured gain for the compact LPDA on Duroid and FR4 substrates.

The different configurations of the planar LPDA were evaluated through measurement, where it was determined that any variations found were negligible. The difference in configurations involved how the feed point at the top of the planar LPDA was fabricated as well as rounding the corners of the dipole elements to remove unwanted electric current discontinuities. The best design was found to be an insulated cable running along the center trace with a through-hole for the center conductor and the cable shield connected only at the end of the center trace. The simulated and measured reflection coefficient are shown in Fig. 8 for the planar LPDA with the feed model shown in the inset figure. Only 8 mm of the coaxial cable with waveguide port is included in the simulation where the solid center conductor extends 1.7 mm beyond the cable shield with right angle bend.

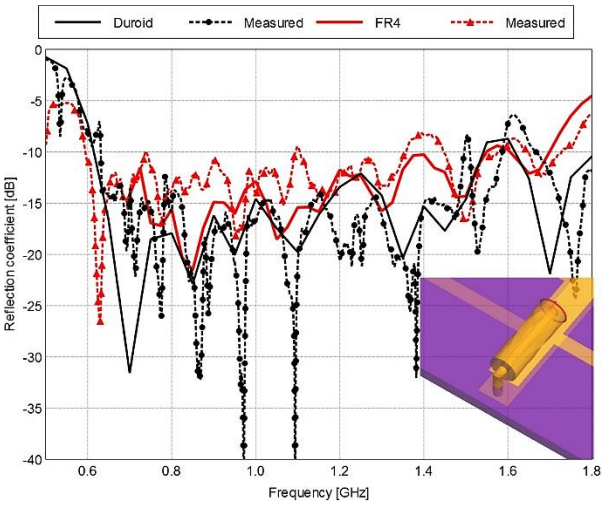

Fig. 8. Planar LPDA reflection coefficient comparison for Duroid and FR4.

The comparison shows relatively good agreement between simulation and measurement. The measurement also shows that the FR4 is not as well matched as the Duroid. The E-plane patterns at 900 MHz are shown in Fig. 9 where, with Duroid substrate, the gain is 7.7 dBi compared to 6 dBi using FR4, confirming that the dielectric losses reduce the antenna efficiency.

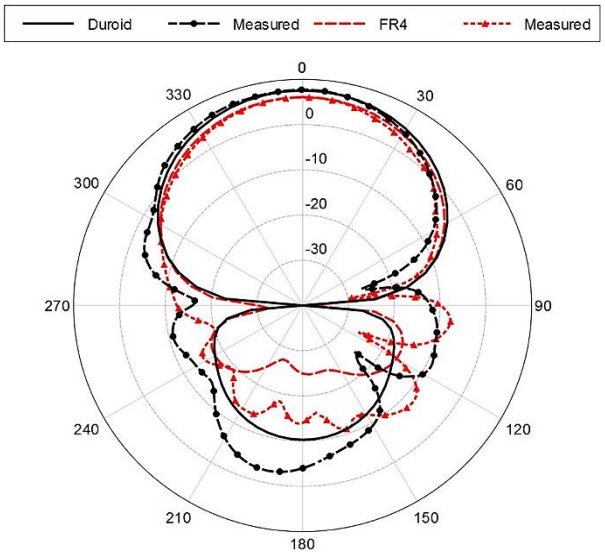

Fig. 9. Planar compact LPDA E-plane comparison for Duroid and FR4 substrates.

III. ARRAY MEASUREMENTS

The planar LPDA elements are matched over the frequency band 800 to 1,300 MHz. The array spacing was chosen to be a half-wavelength centered in that band, i.e., 1,075 MHz 139.5 mm (5.49 in.). The planar LPDA elements are oriented at 45° (slant-polarization) in order to transmit both horizontal and vertical field components with respect to the ground.

The 8-element horizontal array provides high gain (15.5 dBi), electronic scanning, and a narrow beam in azimuth (14.6°) with broad beamwidth in elevation. With this design, the maximum array width is 1.25 m with a maximum height of 0.68 m. The planar LPDAs are mounted inside a plastic enclosure with a polycarbonate radome (1/8 in. thick) on the enclosure front which is then mounted to a metal enclosure housing the amplifiers and phase shifters.

The model used for in-situ simulations is shown in Fig. 10. The presence of the metal electronics enclosure has only a small influence on the forward gain. Note that the plastic enclosures were not meshed for simulation and are only kept to maintain proper antenna placement when adjusting element positions. Measurements with and without the polycarbonate radome indicate negligible difference. The elements use simple edge ports instead of the coaxial wave port feed for efficient computation.

The simulation for 8-elements without substrates at 3 m above a lossy half space (ε_r = 10, σ = 5 mS/m) required only 450 MB and 90 s/frequency on 4 CPUs. Including the substrates was a severe computational penalty requiring 132 GB and 17.5 hours per frequency on 16 CPUs. The lossy half space was modeled using the infinite half space dielectric in FEKO. The fields in the half space are computed by solving the exact Somerfield integral equations in the media. While slower to compute than the reflection coefficient approximation, the results are more akin to the real world. Simulations showed that pattern perturbations in the azimuthal plane are negligible, and that there is interference in the elevation plane due to ground bounce.

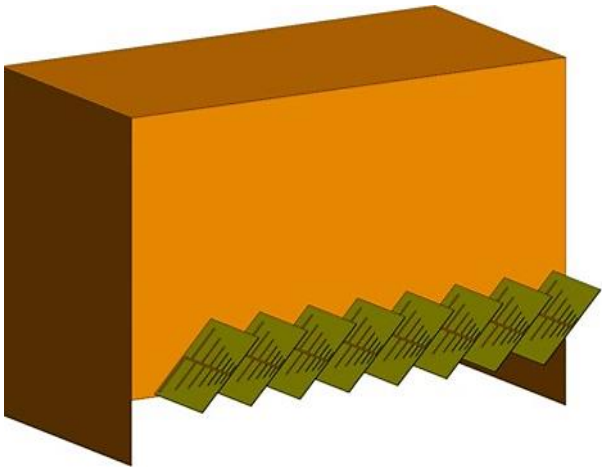

Fig. 10. In-situ model for 8-element horizontal array on metal enclosure located at 3 m above soil.

The comparison between simulation and measurement for in-phase antenna elements is shown

in Fig. 11. Scanning was implemented and tested using 8 voltage controlled phase shifters. The data was taken over a ±90° span in azimuth to prevent damage to the input cable during rotation. Figure 11 shows that the peak gain and beamwidth are as expected with the first null occurring at ±18° from boresight. The simulation is in good agreement with some minor asymmetries in the measured sidelobes. These asymmetries are associated with differences in the polarization dependencies of the chamber since slant polarization is used in the chamber measurements. In particular, asymmetries due to wall side vs. door side.

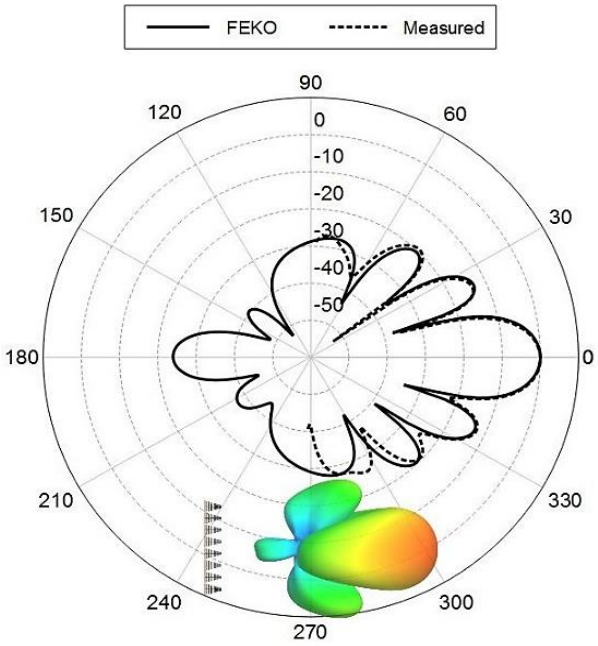

Fig. 11. 8-element horizontal array normalized azimuthal pattern comparison at 900 MHz.

Figures 12 and 13 show the raw measured azimuthal pattern when scanning at 900 and 1,300 MHz respectively. The legend gives the phase progression used to scan to the associated azimuth positions. The asymmetric decrease in beam peak from scanning the array to one side and then to the other is most likely due to the measurement environment where there can be asymmetries due to absorber placement (door side versus wall side) with differences between horizontal and vertical polarization.

The inconsistency in beam location between 900 and 1,300 MHz is expected from array theory, where the phase progression is frequency dependent and would need compensation at 1,300 MHz to scan to the same position as the 900 MHz case. The measured results conclude that the scanning configuration is a success, but care would need to be taken when setting the phase progression to make sure that the array scans to the correct location.

Accomplishing the secondary function, where both a wide beam and high gain are required, necessitated splitting the 8-element array into two 4-element horizontal arrays. Initial hypothesis supposed pointing the main beam of each subarray towards the 3 dB beamwidth location (7°) of the uniform 8-element array azimuthal pattern would achieve a broad beam. But further study showed that it is preferred to phase the two 4-element subarrays so as to point just past the first nulls instead (at 20° from boresight).

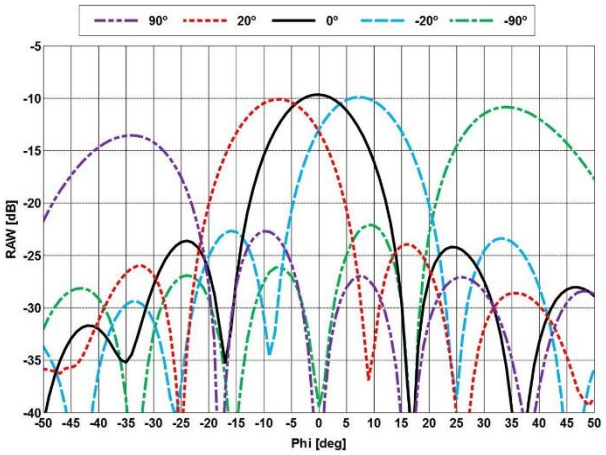

Fig. 12. Electronically scanned 8-element array raw patterns at 900 MHz.

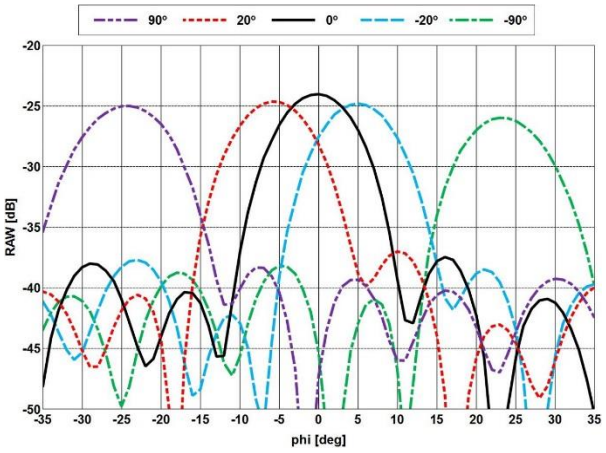

Fig. 13. Electronically scanned 8-element array raw patterns at 1,300 MHz.

The 4-element E-plane patterns are shown in Fig. 14 (left) when pointed at 17° resulting in a peak gain of 11.8 dBi. Figure 14 (right) shows the combined subarray pattern for 7°, 20°, and 24° beam peak location. It was found that pointing these subarrays at 20° off boresight provided a larger beamwidth with ~1.5 dB less gain compared to pointing at the 17° null locations. Scanning the subarrays to 7° produced little change in the

beamwidth and gain, and scanning the beam to the actual null location does not give the desired beamwidth. The best results occurred when the subarrays were pointed slightly past the nulls at 20°. Pointing the subarrays past 20° results in a significant decrease in broadside gain.

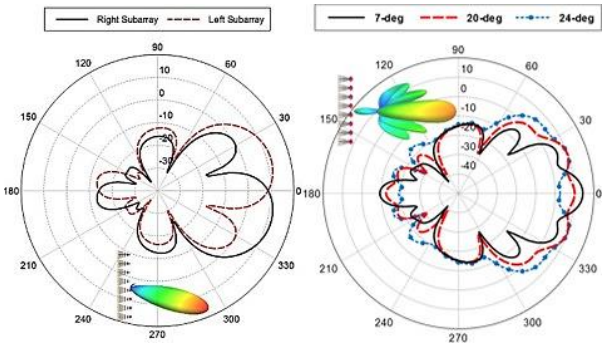

Fig. 14. 4-element subarrays simulated azimuthal patterns pointed at 17° (left) and combined subarrays with scan angles of 7°, 20°, and 24° (right) at 900 MHz.

The simulated and measured azimuthal pattern for subarrays pointed at 17° and 20° is shown in Fig. 15, indicating a 10.1 dBi boresight gain with the second peak at 9.8 dBi and the larger beamwidth for 20°. The simulated results show that pointing the subarrays slightly past the null location gives the best results. This approach provides the desired 55° beamwidth with gain ~1 dB less than a single 4-element subarray. This pattern could be continually scanned over ±12° to provide somewhat higher gain over the forward sector as shown in Fig. 16. Then having high gain covering the forward sector would depend on the scan rate which would be application specific.

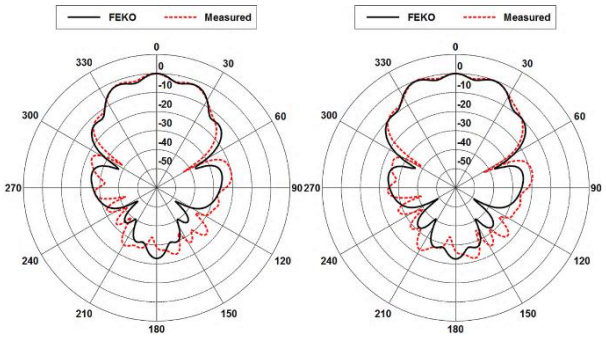

Fig. 15. Combined 4-element subarray azimuthal pattern comparison with scan angle of 17° (left) and 20° (right) at 900 MHz.

Validation of the subarrays was performed as shown in Fig. 17. Both the left and right subarrays show good agreement with simulation, with the difference in forward gain being the exclusion of the FR4 substrate from simulation. The removal of the substrate was done to minimize the required system memory and computational time. Again, there are some slight asymmetries between the left and right subarrays which is due to the measurement environment.

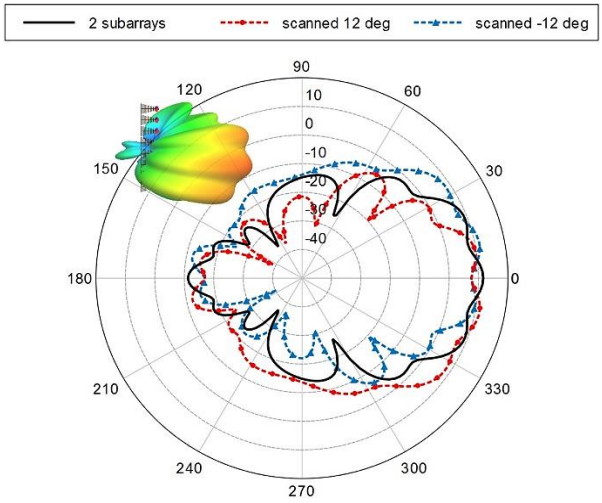

Fig. 16. Scanned null-filled azimuthal patterns at 900 MHz.

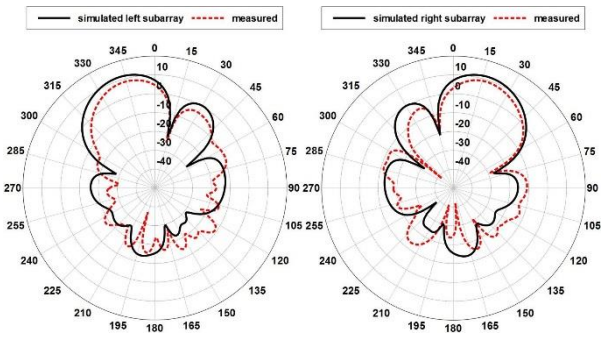

Fig. 17. Simulated and measured left and right subarray azimuthal pattern comparison at 900 MHz.

Measurements at 850 MHz and 950 MHz for the combined null filled pattern showed that the beamwidth will decrease with increasing frequency. This is to be expected as the element spacing and phase progression are frequency dependent, meaning that some loss of beamwidth will inevitably occur. The element pattern is not a cause of the decreasing beamwidth, as the gain has already been shown to be relatively flat with increasing frequency.

IV. CONCLUSION

This paper has presented the design, simulation, and measurement of a dual use 8-element horizontal array and its individual planar LPDA elements for the frequency band of 800 to 1300 MHz. A typical LPDA was scaled to be more compact than a traditional design

with little impact on performance. Modifications to the compact LPDA allow the antenna to be fed from the rear rather than the front, but care had to be taken to make sure that the coaxial cable was well insulated from the center trace. If the cable was attached to this trace then performance degradation would occur.

The dual use 8-element horizontal array was designed to transmit (receive) slant-polarization. In one configuration, the array needed to be able to scan in azimuth with a narrow beam, and in the other configuration, needed to maximize azimuthal beamwidth and forward gain. The second configuration was accomplished through null filling in which the 8-element array was divided into two 4-element subarrays. The beam of each subarray was scanned just past the associated first null of the broadside 8-element azimuthal pattern. The combined subarray pattern produced an azimuthal beamwidth of 55° (versus 15° for 8-elements) with 10 dBi of gain (versus 15 dBi for 8-elements). The measurements in a tapered anechoic chamber for the array in both configurations and for a single antenna element are in good agreement with simulation, thereby confirming proper function of this array designed by simulation.

REFERENCES

[1] J. A. Rodriguez and F. Ares, "Synthesis of shaped beam antenna patterns with null filling in the sidelobe region," *IEEE Electronic Letters*, vol. 33, no. 24, pp. 2004-2005, November 1997.

[2] D. Shin, et al., "Design of null filling antenna for automotive radar using the genetic algorithm," *IEEE Antennas and Wireless Propagation Letters*, vol. 13, pp. 738-741, 2014.

[3] FEKO, ver. 14.0.401, Altair, Troy, MI, 2016.

[4] C. Peixeiro, "Design of log-periodic dipole antennas," *IEE Proceedings*, vol. 135, no. 2, pp. 98-102, April 1988.

[5] W. L. Stutzman and G. A. Thiele, *Antenna Theory and Design*. John Wiley & Sons, New Jersey, 2013.

[6] GEMS, ver. 7.90.21, 2COMU, Inc., Fairfax, VA, 2014.

Seth A. McCormick received his BS. in Electrical Engineering in 2014 and is currently pursuing a MEE from Virginia Polytechnic Institute. He currently works as an Electronics Engineer for the Army Research Laboratory (ARL). Prior to that, he was a Contractor with General Technical Services LLC at ARL. As a member of the antenna team under the Sensors and Electron Devices Directorate, he uses several CEM codes for the design and modeling of antennas and for general EM analysis. His primary research interests are in antenna design and analysis, CEM, electromagnetic materials, and electromagnetic theory. He is a Member of ACES and a Student Member of Sigma Xi. He has authored or coauthored 11 publications.

William O. Coburn received his BS in Physics from Virginia Polytechnic Institute in 1984. He received an MSEE in Electro Physics in 1991 and Doctor of Science in Electro-magnetic Engineering from George Washington University (GWU) in 2005. His dissertation research was in traveling wave antenna design. He has 36 year's experience as an Electronics Engineer at the Army Research Laboratory (formerly the Harry Diamond Laboratories) primarily in the area of CEM for EMP coupling/hardening, HPM, target signatures and antennas. He currently is in the RF Electronics Division of the Sensors and Electron Devices Directorate applying CEM tools for antenna design and EM analysis. He is a Senior Member of the IEEE, APS Society and Fellow of the Applied Computational EM Society (ACES) serving on the ACES Board of Directors. He is a Member of the USNC-URSI, Commission A and B (2010), *Sigma Xi* and an Adjunct Professor at the Catholic University of America. Coburn has authored or coauthored about 45 publications and 4 patents.